HHS Public Access

Author manuscript

Spine J. Author manuscript; available in PMC 2016 June 07.

Published in final edited form as:

Spine J. 2012 January ; 12(1): 7–20. doi:10.1016/j.spinee.2011.09.011.

Injection of AAV2-BMP2 and AAV2-TIMP1 into the nucleus pulposus slows the course of intervertebral disc degeneration in an in vivo rabbit model

Steven K. Leckie, MD[*], **Bernard P. Bechara, MSc**, **Robert A. Hartman, MSc**, **Gwendolyn A. Sowa, MD, PhD**, **Barrett I. Woods, MD**, **Joao P. Coelho, MSc**, **William T. Witt, MSc**, **Qing D. Dong, MSc**, **Brent W. Bowman, BA**, **Kevin M. Bell, MSc**, **Nam V. Vo, PhD**, **Bing Wang, MD, PhD**, and **James D. Kang, MD**

Department of Orthopedic Surgery, University of Pittsburgh Medical Center, BST E1641, 200 Lothrop St, Pittsburgh, PA 15213, USA

Abstract

BACKGROUND CONTEXT—Intervertebral disc degeneration (IDD) is a common cause of back pain. Patients who fail conservative management may face the morbidity of surgery. Alternative treatment modalities could have a significant impact on disease progression and patients' quality of life.

PURPOSE—To determine if the injection of a virus vector carrying a therapeutic gene directly into the nucleus pulposus improves the course of IDD.

STUDY DESIGN—Prospective randomized controlled animal study.

METHODS—Thirty-four skeletally mature New Zealand white rabbits were used. In the treatment group, L2–L3, L3–L4, and L4–L5 discs were punctured in accordance with a previously validated rabbit annulotomy model for IDD and then subsequently treated with adeno-associated virus serotype 2 (AAV2) vector carrying genes for either bone morphogenetic protein 2 (BMP2) or tissue inhibitor of metalloproteinase 1 (TIMP1). A nonoperative control group, nonpunctured sham surgical group, and punctured control group were also evaluated. Serial magnetic resonance imaging (MRI) studies at 0, 6, and 12 weeks were obtained, and a validated MRI analysis program was used to quantify degeneration. The rabbits were sacrificed at 12 weeks, and L4–L5 discs were analyzed histologically. Viscoelastic properties of the L3–L4 discs were analyzed using uniaxial load normalized displacement testing. Creep curves were mathematically modeled according to a previously validated two-phase exponential model. Serum samples obtained at 0, 6, and 12 weeks were assayed for biochemical evidence of degeneration.

RESULTS—The punctured group demonstrated MRI and histologic evidence of degeneration as expected. The treatment groups demonstrated less MRI and histologic evidence of degeneration

[*]Corresponding author. Department of Orthopedic Surgery, University of Pittsburgh Medical Center, BST E1641, 200 Lothrop St, Pittsburgh, PA 15213, USA. Tel.: (412) 648-1090. ; Email: leckiesk@upmc.edu (S.K. Leckie)

FDA device/drug status: Not applicable.

Author disclosures: SKL: Nothing to disclose. BPB: Nothing to disclose. RAH: Nothing to disclose. GAS: Nothing to disclose. BIW: Nothing to disclose. JPC: Nothing to disclose. WTW: Nothing to disclose. QDD: Nothing to disclose. BWB: Nothing to disclose. KMB: Nothing to disclose. NVV: Nothing to disclose. BW: Nothing to disclose. JDK: Nothing to disclose.

than the punctured group. The serum biochemical marker C-telopeptide of collagen type II increased rapidly in the punctured group, but the treated groups returned to control values by 12 weeks. The treatment groups demonstrated several viscoelastic properties that were distinct from control and punctured values.

CONCLUSIONS—Treatment of punctured rabbit intervertebral discs with AAV2-BMP2 or AAV2-TIMP1 helps delay degenerative changes, as seen on MRI, histologic sampling, serum biochemical analysis, and biomechanical testing. Although data from animal models should be extrapolated to the human condition with caution, this study supports the potential use of gene therapy for the treatment of IDD.

Keywords

Intervertebral disc degeneration; Gene therapy; BMP; TIMP

Introduction

Spine clinicians are frequently called on to treat intervertebral disc degeneration (IDD). The back pain associated with IDD dramatically affects patients' quality of life and work productivity and significantly impacts health care spending. Of all physician visits, 12% to 15% are because of back pain, and 20% of the patients report that they cannot work as a consequence of their back pain [1]. From 2002 to 2004, the annual cost for spine-related pain exceeded $30 billion in direct medical costs and more than $14 billion in lost wages [1].

Disc degeneration is associated with spinal stenosis, facet hypertrophy, herniation, and other pathology that may engender symptoms. The current treatment paradigm starts with activity modification, analgesic and anti-inflammatory medications, and physical therapy. Although many patients will respond to conservative treatment, patients who fail may be surgical candidates [2]. Surgery does not reliably improve discogenic low back pain. Furthermore, surgery entails risks, demands convalescence, and worsens degeneration at adjacent levels [3]. Less invasive treatment paradigms that can safely and effectively alter the course of IDD without hindering motion could have a significant impact on the lives of millions of patients.

Discs degenerate through a complex biochemical cascade. The intervertebral disc (IVD) is largely avascular. Nutrition and oxygenation rely on passive diffusion, sometabolism at the center of the disc is mostly anaerobic [4]. Lactate production generates an acidic pH, which creates a biologically harsh environment. Because of avascularity, low oxygen tension, acidic pH, sparse cellularity, and limited nutrition, the disc has a very poor healing capacity [5]. With degeneration, the disc undergoes complex biochemical and biomechanical changes that involve a progressive loss of proteoglycan content, leading to dehydration of the nucleus pulposus (NP) [6]. As the desiccating disc loses its turgor pressure and collapses, increased stress is placed on the facet joints, leading to altered biomechanics and arthritic changes [7].

A disruption in normal disc homeostasis leads to an increase in catabolic activity and a decrease in anabolic activity. Bone morphogenetic proteins (BMPs) are anabolic growth factors that play an important role in skeletal development and repair. In cell culture, BMP2,

one of the 20 known BMPs, stimulates chondrocytes to produce proteoglycan [8], directly increases collagen synthesis, and upregulates the expression of other BMPs (such as BMP7) [9]. Meanwhile, tissue inhibitors of metalloproteinases (TIMPs) are anticatabolic growth factors that prevent matrix metalloproteinases from enzymatically cleaving proteoglycans. Tissue inhibitor of metalloproteinase 1 inhibits matrix metalloproteinase 3 in the IVD [10]. Degenerated human IVDs cultured from discectomy patients demonstrate an increase in total proteoglycan when transfected with adenovirus (Ad) carrying either BMP2 or TIMP1 [11] because BMP2 stimulates proteoglycan synthesis and TIMP1 inhibits metalloproteinase from degrading the extracellular matrix. The success of Ad-BMP2 and Ad-TIMP1 in vitro makes these genes attractive candidates for in vivo investigation. Adenovirus is a potent transducer, but it can cause a catastrophic anaphylactic response. It can also cause local toxicity if misinjected into the cerebrospinal fluid. In an in vivo experiment using both monkeys and rats, Ad was purposefully injected through the dura into the cerebrospinal fluid. This resulted in histopathologic changes consistent with viral meningitis, an immune response, and symptoms of lethargy and weight loss [12]. Adeno-associated virus (AAV) is a vector that is capable of efficiently transducing human and rabbit IVDs in vitro and in vivo. It demonstrates a superior safety profile to Ad vectors when purposefully misinjected into the epidural space [13]. Although it can elicit a humoral immune response, transgene expression is feasible even in pre-exposed animals [14]. Viral attenuation by the immune response can be overcome by increasing the dose of viral particles, number of cells infected, and amount of time between initial antigen sensitization and transgene injection [15]. Adeno-associated virus is not associated with any pathologic conditions in humans, although up to 90% of people older than 50 years have developed antibodies against the wild-type virus [16].

This study investigates the utility of gene therapy to improve IDD by introducing anabolic (BMP2) and anticatabolic (TIMP1) growth factors into disc cells via a safe viral vector (AAV serotype 2 [AAV2]). To our knowledge, AAV2-BMP2 and AAV2-TIMP1 have not been tested in an in vivo disc degeneration model. Annulotomy of a rabbit's IVD induces a reproducible cascade of disc degeneration [17]. We used this validated IDD model to determine whether treatment with AAV2-BMP2 or AAV2- TIMP1 can ameliorate the course of disc degeneration. We hypothesized that the extent of disc degeneration in the treated rabbits will be reduced compared with untreated degenerating controls.

Methods

Rabbits Thirty-four healthy skeletally mature New Zealand white rabbits (female, aged 1 year, and weight 5 kg) were divided into five groups: nonsurgical (nondegeneration and negative control, n56), sham surgery (nondegeneration and negative control, n54), puncture surgery (disc degeneration and positive control, n57), punctured followed by AAV2-BMP2 injection (BMP2 treatment group, n58), and punctured followed by AAV2-TIMP1 injection (TIMP1 treatment group, n58) (Fig. 1). We anticipated needing five rabbits per treatment group based on a power analysis of preliminary serum data, and this number was increased to account for possible animal losses. Groups have different numbers of rabbits because of housing constraints and one death that was unrelated to treatment. This study was performed

in full compliance with our Institutional Animal Care and Use Committee guidelines, approved protocol 0809294.

Sample preparation

The transfection systems AAV2-BMP2 and AAV2-TIMP1 were developed by author BW. Both plasmid DNA constructs of recombinant AAV vectors, pAAV-CMV-hBMP2 and pAAV-CMV-hTIMP1 were regulated by the human cytomegalovirus (CMV) immediate-early promoter/enhancer and followed by the simian virus 40 polyadenylation signal from the simian virus 40 genome. One was designed to express human BMP2in a single-stranded AAV vector, and another was structured to express human TIMP1 in a self-complementary AAV vector (Fig. 2). The plasmid DNAs were purified twice by the cesium chloride gradient ultracentrifugation processes according to the standard protocol. The Serotype 2 of both AAV-CMV-hBMP2 and pAAV-CMV-hTIMP1 viruses was generated precisely by the triple plasmid cotransfection of human embryonic kidney 293 cells as described by Xiao et al. [18]. The AAV vectors were subsequently purified twice through cesium chloride density gradient ultracentrifugation using previously published protocols [19]. The vector titers of viral genome number were detected by DNA dot blot method and were approximately within 5_1012 to 1_1013 viral genome number per milliliter [20].

Puncture surgery

Disc degeneration was induced via a validated rabbit puncture model [21]. This injury model initiates a reliable cascade of magnetic resonance imaging (MRI) and histologic changes that resemble the hallmarks of human disc degeneration (darkening and collapse of disc spaces). Under sterile surgical conditions and general anesthesia, the rabbits' spines were exposed from an anterolateral retroperitoneal approach. L4–L5, L3–L4, and L2–L3 discs were sequentially punctured with a 16-gauge needle to a depth of 5 mm (parallel to the end plates [EPs], such that the tip of the needle was in the center of the NP), and then the surgical incisions were closed and standard postoperative care was performed. In the sham group, the discs were exposed but not punctured, and the surgical incisions were subsequently closed. In the nonoperated control group, the rabbits underwent no surgical intervention. Postoperatively, the rabbits were housed in individual cages and permitted food and activity ad lib.

Injection surgery

Sixteen operative rabbits returned to surgery 3 weeks status postpuncture surgery. This time point was selected because 3 weeks is the earliest that MRI changes of degeneration have been detected with this model [21], and the goal of gene therapy is to intervene early while the discs still have the metabolic capacity to alter the course of degeneration. L4–L5, L3–L4, and L2–L3 discs were approached from the right side (contralateral to the previous puncture surgery). A Hamilton 100-mL syringe (1710TPLT; product #81041) and a Hamilton 30-gauge sharp-tipped needle with a plastic hub (KF730 NDL 6/pack, 30G/200; product #90130) were used for therapeutic injections into the center of the NP (Hamilton, Reno, NV, USA). The small needle size was selected such that it would not exacerbate further degeneration [22]. Each disc was injected with 108 virus particles (either AAV2-BMP2 or

AAV2- TIMP1) in 15 mL of sterile saline steadily over the course of 1 minute. This quantity was based on previously published dosing [14]. Prior studies proved that the small diameter needle and the effect of injecting a small volume of saline [23], or a nontherapeutic gene [24], do not induce disc degeneration.

Magnetic resonance imaging

Sagittal MRIs were obtained at Time 0 (before annular puncture), 6 weeks postpuncture, and 12 weeks postpuncture (before sacrifice) for 19 of the 34 rabbits (control [n53], sham [n54], puncture [n54], BMP2 [n54], and TIMP1 [n54]).A3-T Siemens magnet and standard human knee coil were used to obtain T2-weighted images (repetition time53,800 ms, echo time [TE]5114 ms, slice thickness50.6 mm) and T2 mapping images (repetition time51200 ms, TE512, 24, 36, 48, and 60 ms, slice thickness 51.0 mm). The rabbits were sedated and placed in the knee coil in the supine position. The T2-weighted images were used to quantify the amount of degeneration in the discs. The midsagittal image of the T2-weighted MRI was identified based on the width of the vertebral body, spinal cord, and spinous processes. A previously validated automated segmentation method was used in which a computer program identified the signal intensity isolines of the disc and adjacent vertebrae and generated a contour map of the NP [25]. The largest closed area between two adjacent vertebrae represents the NP and was selected as the region of interest (ROI) (Fig. 3). The MRI index is the sum of pixel area multiplied by pixel intensity for all identified NP tissues. The location of the segmented NP from the T2-weighted images was used to identify the location of the NP in the T2 mapping images. The signal exponential decay value (T2 value) of each pixel in the ROI was calculated:

$$\log(I)=\mathrm{A}-\frac{\mathrm{TE}}{\mathrm{T2\ value}}$$

where I is the intensity of the pixel, and TE is the echo time. The T2 value was calculated from five different TEs (12, 24, 36, 48, and 60 ms). After calculating the T2 values, the intensity of each pixel in the ROI was replaced by its respective T2 value, and thus a T2 map was generated. The slope of the T2 map was calculated by plotting the radial distance from the geometric center of the map with the T2 value for each pixel.

Serum

Serum was collected from 15 rabbits (control [n53], puncture [n54], AAV2-BMP2 [n54], AAV2-TIMP1 [n54]). Blood samples were collected at time 0 (before puncture surgery), 6 weeks, and 12 weeks (before sacrifice). The central auricular vein of the ear was used (saphenous vein was occasionally used when ear stick failed). At the 12-week time point (before sacrifice and while the rabbit was anesthetized), a cardiac stick was used. In a tiger topped tube, 2 mL of blood was collected and centrifuged at a rate of 2,000 rpm for 5 minutes. The serum was siphoned off and stored at _80_ within 3 hours of the initial blood draw. Serum samples were banked at _80_ until analysis. Samples were analyzed with a commercially available enzyme-linked immunosorbent assay (Nordic Biosciences, Herlev, Denmark) specific to C-telopeptide of collagen type II (CTX-II), a marker previously shown to increase in this animal model of degeneration [26]. All samples were run in duplicate.

Sacrifice and histologic processing

All rabbits were sacrificed 12 weeks after the initial puncture surgery (after the final MRI and blood samples were obtained). Immediately after death, the spines were dissected out en bloc. The L4–L5 disc was prepared for histologic analysis. The discs were fixed and decalcified with Decalcifier I for 2 weeks and then dehydrated in histology tissue processor and embedded in paraffin. Next, the discs were sectioned at a thickness of 5 mm in the sagittal plane. The sections were stained with hematoxylin and eosin (Fisher Scientific Co., Kalamazoo, MI, USA), using standard histology protocol, and photographed using a Nikon E800 microscope (Nikon Inc. Instrument Group, Melville, NY, USA).

Biomechanics

Functional spinal units (FSUs) for 15 rabbits (control [n53], puncture [n54], BMP2 [n55], TIMP1 [n53]) were cleaned of posterior elements, potted in epoxy resin (Bondo; 3M, Inc., St Paul, MN, USA), and mounted with custom fixtures in an axial testing machine composed of a uniaxial load cell (MLP-100; Transducer Techniques, Inc., Temecula, CA, USA), linear actuator (D-B.125-HT23E10Diff-4-1/4; Ultra Motion, Cutchogue, NY, USA), and microcontroller (Micro- Lynx-4; Schneider-Electric Motion USA, Inc., Marlborough, CT, USA) (Fig. 4) controlled in Matlab (Matlab R2008a; The Mathworks, Inc., Natick, MA, USA). Specimens were kept hydrated at room temperature and surrounded by saline-soaked gauze. Vernier calipers were used to measure the lateral (DLat) and anteroposterior (DAP) dimensions of the disc to obtain a cross-sectional area estimate: A5p/4(DAP_DLat). The relation of P5F/A then prescribed an applied axial force magnitude to attain 1.0 MPa. Preliminary intradiscal pressure experiments showed that this method generated initial pressures within 20% of the 1.0-MPa target. Pressure-target loading allows more consistent correlation with human loading as it accounts for size disparity between species [27]. A 1.0-MPa magnitude is comparable to human standing or vigorous jogging [28]. Specimens were preconditioned with 20 cycles of compressive loading (0–1.0 MPa, 0.1 mm/s), shown in preliminary testing to yield a stable force-displacement response, and then were subjected to constant compression for 1,100 seconds.

The stiffness (newtons per millimeter) of the ramp phase, defined by the time before force target attainment (3–5 seconds), was calculated in the linear region of each force-displacement curve. Average curves were then generated for each condition by individual curve fitting of each test and averaging discrete points along each fit. The creep phase of the curve was defined by the time after the desired force target. To analyze viscoelastic behavior, creep curves were fit with a two-phase exponential model that has been validated in describing motion segment creep [29]:

$$\frac{d(t)}{L_0}=\frac{1}{S_1}(1-e^{-S_1 t/\eta_1})+\frac{1}{S_2}(1-e^{-S_2 t/\eta_2})$$

where d(t) is the axial displacement over time, and L0 is the applied axial force. h represents the viscous component of the viscoelastic response. Proteoglycan content, tissue hydration, and fluid exudation through the collagen proteoglycan matrix are thought to govern the viscous parameters. The elastic component of the viscoelastic response is represented by S.

The collagen network is believed to govern the elastic parameters [30]. Subscript 1 denotes the early response and 2 denotes the late response. The early viscous (h1) and early elastic (S1) responses are thought to be determined by the NP, whereas the late viscous (h2) and late elastic (S2) responses are thought to be determined by the annulus fibrosus (AF) [29]. Curve fitting was performed in Matlab using a trust-region algorithm with starting guesses and boundaries derived from a previous rabbit study [29]. Starting guess combinations (n52,500), where each parameter's starting guesses spanned an order of magnitude, were used for each condition's average curve. Resulting parameter sets whose correlation coefficient (R2) exceeded 0.95 were included. Calculations were made from average curves, and quantified trends are reported.

Results

Rabbits

There was one perioperative death during puncture surgery because of a complication from anesthesia. Several rabbits chewed at their surgical incisions, which were managed with local wound care. There were no adverse events noted in any of the treatment rabbits that could be attributed to the therapeutic injection. All rabbits appeared to behave normally after treatment.

Imaging

Lateral lumbar spine X-rays obtained at time 0 and 12 weeks did not demonstrate osteophytes or abnormal bone growth in any of the groups (images not shown). As shown in Fig. 5, qualitative inspection of the T2-weighted midsagittal MRIs of the nonoperative control group (and sham group, not shown) did not undergo any MRI evidence of disc degeneration. Nucleus pulposus images from the punctured group darkened and decreased in area from 0 to 12 weeks, consistent with degeneration. Both treatment groups demonstrated less qualitative evidence of degeneration than the punctured group (the treated NPs retain their size and do not darken as much as the punctured discs). The percentage NP area and MRI index relative to Week 0 for each group were averaged across the three discs of interest and plotted versus time in Fig. 6. The control and sham groups were not significantly different at any time point. The NP area decreased similarly across time points for the punctured group and the two treatment groups, but the MRI index decreased less for the two treatment groups compared with the punctured group. At Weeks 6 and 12, the NP area was smaller for the punctured group and the two treatment groups compared with the control and sham groups. The difference in the NP area between BMP2 and control at Week 6 was statistically significant (p!.05). Similarly, at Week 12, the difference between punctured and control, BMP2 and control, and TIMP1 and control was statistically significant (p!.05). At Week 6, the difference in MRI index between the TIMP1 and puncture groups was statistically significant (p!.05). At 12 weeks, there was a significant difference in MRI index between control and puncture and between control and the treated groups. Although the difference between puncture and the treated groups' MRI indices did not achieve statistical significance at 12 weeks, both treated groups fell between the punctured (most degenerated) and control/sham (nondegenerated) states.

The T2 maps at 12 weeks depict a difference between the groups (Fig. 7); the control discs have a high and narrow appearing map (indicating a heterogeneous pixel distribution), whereas the punctured discs have a low and wide map (representing a more homogeneous pixel distribution). The treated groups have disc maps that fall between the punctured and nonpunctured control maps, with the BMP2-treated groups appearing more like control discs and the TIMP1-treated discs appearing more like punctured discs.

These differences were quantified by calculating the height of the map relative to the distance from the center of the disc, thereby generating a map slope. Because the T2 values decreased with radial distance from the center, the slope is negative, but for illustration purposes, Fig. 8 shows the average of the absolute value of the slope across discs for each group. As shown in the figure, the slope of the punctured group decreased with time more than the control group. The sham group followed the control group, with the exception of some divergence at 12 weeks. Meanwhile, the treated groups generated an average slope that fell between the punctured and nonpunctured controls. The slope of the punctured group was statistically different (p!.05) than the control group at both 6 and 12 weeks. As with the MRI index data, at Week 6, the difference in map slope between TIMP1 and the punctured group was statistically significant (p!.05). Otherwise, treated map slopes fell between the punctured and control values but did not achieve statistical significance.

Serum

The CTX-II concentration was determined for each group at 0, 6, and 12 weeks. The untreated punctured rabbits had a significantly higher CTX-II concentration in comparison to all of the other groups at 12 weeks postpuncture (p!.05). The CTX-II increase, which was observed in the punctured animals, was blunted by either AAV2-BMP2 or AAV2-TIMP1 treatment, which was similar to the CTX-II concentration of the controls at 12 weeks (Fig. 9).

Biomechanics

The L3–L4 motion segments underwent cyclic preconditioning and constant axial compression. Total load normalized displacements are given in Fig. 10. From these average curves, differences between conditions are apparent. Control and TIMP1 discs generate curves that fall between punctured and BMP2 discs. Differences in ramp phase stiffness are evident in the Table; BMP2-treated discs have stiffnesses that are similar to controls, and TIMP1- treated discs are similar to punctured discs. Model coefficients, depicted in the Table, describe differences in creep behavior between groups. Elastic damping coefficients, S1 and S2, are each reduced in the punctured group by 12%. BMP2 treatment increases S1 and S2 values by 44% and 32% relative to punctured values, whereas TIMP1 treatment has less of an effect (10% and 3% increase relative to punctured values). Early viscous damping coefficients (h1) exhibit the same trend between experimental groups; that is, the punctured group is slightly decreased relative to control (10%), TIMP1 is moderately increased (11%), and BMP2 is markedly increased (118%) relative to punctured. Late viscous damping coefficients (h2) evidence little difference between control and punctured discs, with 15% increase in BMP2-treated discs and 6% decrease in TIMP1-treated discs relative to control discs. Histology

Midsagittal cuts of hematoxylin and eosin–stained L4–L5 disc in the punctured group demonstrate a range of degenerative changes from partial to complete loss of the NP with fibrosis and loss of cellularity. Punctured discs have a fibrocartilaginous AF matrix with disorganized lamellae. Compared with the control and sham groups, punctured discs demonstrate evidence of degeneration. Treatment with AAV2-BMP2 or AAV2-TIMP1 demonstrates relative preservation of NP area, architecture, and cellularity, although some fibrosis is observed (Fig. 11). There was no histologic evidence of abnormal bone growth in any of the groups.

Discussion

For the first time to our knowledge, we have shown that AAV2-BMP2 and AAV2-TIMP1 injection into the IVD could ameliorate the course of IDD in vivo. Both interventions demonstrated slowing of the course of injury-induced degeneration according to MRI, histologic, serum biomarker, and biomechanical criteria. T2-weighted MRI trended toward relative preservation of the signal intensity and T2 map compared with punctured animals. C-telopeptide of collagen Type II, a promising new biomarker, was released into the serum in significantly lower quantities of animals treated with either therapeutic gene compared with the degenerated state. Treatment also induced a trend toward normal disc cellularity and architecture on histologic analysis. Finally, a difference was detected in the way the treated FSUs behave under physiologic axial loading conditions. Although not all findings were statistically significant, consistent trends were demonstrated. This study is unique in that it includes a broad and diverse range of outcome measures, including serum biomarkers, novel MRI technology, and biomechanics, not only to quantify IDD but also more importantly to show a response to a targeted treatment for disc degeneration with the AAV vector. These data provide exciting new evidence to justify further exploration of gene therapy using these candidate genes to treat disc degeneration.

Rabbits and surgical degeneration model

Although an injury model for disc degeneration does not truly reflect the complex biochemical cascade of human degenerative disc disease, it does show that intradiscal injection of AAV2-BMP2 and AAV2-TIMP1 is a feasible treatment method to slow the process of injury-induced degeneration. The puncture model does not cause extrusion of NP but rather seeks to induce an injury response that maintains the contents of the NP so that there is substrate on which the treatment injections can work. The timing of the treatment injections is purposefully early in the degeneration cascade, as further progression of cellular changes could reach a burned-out state from which the host environment might no longer be able to mount a healing response. However, intervention at a later time point would also be worth investigating because of the clinical relevance of later disease detection.

Gene therapy

Prior in vivo studies using growth factors alone (as opposed to incorporated into a viral vector) for the treatment of IDD have yielded encouraging results. In the rabbit annular puncture model, injection of recombinant human BMP7 restored the biochemical and histologic integrity of degenerating discs [31]. This therapeutic effect of BMP7 was also

noted after administration to discs that had undergone degeneration caused by chemonucleolysis [32].

Other studies on gene therapy for the treatment of IDD have demonstrated efficacy. Lim mineralization protein 1 (LMP1) is an upstream regulator of multiple BMPs. Rabbit IVD cells transduced with Ad carrying LMP1 increased expression of BMP2, BMP7, aggrecan, and glycosaminoglycan (which are major constituents of proteoglycan). This in vitro analysis was then translated to the in vivo condition by injecting the Ad-LMP1 vector into rabbit IVDs with similar positive results [33]. Other growth factors, such as transforming growth factor b1 carried by Ad [34], have also demonstrated efficacy at inducing proteoglycan synthesis in vivo.

There are other examples of successful gene therapy for disc degeneration in the literature. Proteoglycan synthesis is increased in the degenerating disc by treatment with transgenic BMP2, LMP1, and TIMP1. Collagen II is increased by transfection of Sox9. Sox9 is an essential transcription factor for chondrocyte differentiation during embryogenesis and for Type II collagen synthesis. Cultured human degenerated IVD cells increased Type II collagen synthesis when transduced with Ad carrying the Sox9 transgene. In the rabbit model for IDD, cells transduced with Ad-Sox9 maintained a chondrocytic phenotype and normal NP architecture compared with degenerating controls [35]. Systems capable of turning on or off with the addition of a ligand add a further degree of control and safety [36].

MRI as an outcome tool

Clinicians who treat human IDD rely heavily on MRI to lend objective evidence to patients' subjective complaints and variable physical examination findings. This study relies on the same MRI evidence of IDD in an animal model in which history and physical examination findings are impossible to obtain. In the clinical setting, spine MRIs are usually evaluated qualitatively, but this study seeks to quantify degeneration as a research tool for comparative purposes. Magnetic resonance imaging changes have been quantified in terms of the area and the MRI index of the NP. These parameters showed a significant and consistent change relative to disc degeneration and were reliable tools to assess the effectiveness of the BMP2 and TIMP1 treatment. Furthermore, MRI index seems to be more sensitive in detecting differences between the various groups. This is shown in Fig. 6 at Week 12 where the puncture, BMP2, and TIMP1 groups had similar areas, although their MRI indices are different. Magnetic resonance imaging–detected degeneration induced by the puncture model has been correlated with disc water and proteoglycan content in the literature [37,38]. T2-weighted MRIs demonstrated that AAV2 injection with either therapeutic gene resulted in no preservation in area compared with puncture alone but did demonstrate a relative preservation of signal intensity, although this only reached statistical significance at the 6-week time point for AAV2-TIMP1. It is possible that the therapeutic effect of delaying matrix breakdown resulted in greater proteoglycan content and water maintenance in the NP and therefore greater signal intensity. It is also possible that the 12-week course of this study may have been insufficient to demonstrate the full therapeutic effect in the degenerative cascade because in this model degeneration has been shown to continue through at least 24 weeks [21], and therefore, longer time points may have demonstrated more statistically

significant changes in signal intensity between treated and punctured discs. It should be noted that even the nonpunctured controls and sham surgery rabbits underwent a modest degree of degeneration. This likely represents natural aging and has been documented previously in nonpunctured rabbits that were followed with serial MRIs for 120 weeks [39].

Serum

Radiographic finding may not always correlate with presenting symptoms [40,41]. Serum biomarkers, especially CTX-II, have shown promise as a potential adjunct to current diagnostic modalities [42–44]. In several other degenerative processes, such as osteoarthritis (OA), there are correlations between the level of serum biomarkers and the severity or progression of disease [45–47]. Serum biomarkers have been found to correlate with disc degeneration as well [48]. In particular, collagen breakdown can be detected in peripheral blood through the measurement of C-telopeptide II, which is a breakdown product from the C terminus of Type II collagen (which is abundant in the NP of the IVD). C-telopeptide of collagen Type II is increased in menopausal woman with disc degeneration, independent of knee and hand OA[49], and has shown promise as a potential biomarker to detect the presence and progression of disc degeneration [50]. The measurement of serum biomarkers such as CTX-II could help assess disc degeneration because serum levels of matrix breakdown products might reflect the presence of active disease or help track disease progression more precisely than can be determined with physical examination and imaging. Importantly, we have previously demonstrated that CTX-II increases significantly in the serum of our animal model of degeneration and changes earlier than imaging findings [24]. Additionally, utilization of this outcome measure could provide molecular metrics of success for novel therapeutics, such as gene therapy, as demonstrated in this study.

The identification of a serum biomarker like CTX-II as a diagnostic adjunct would be an improvement over our current imaging studies alone, which are insufficient to distinguish active disease from age-related asymptomatic changes in humans. In this study, we hypothesized that treating degenerating discs with therapeutic genes would be reflected in CTX-II serum concentrations, thus potentially providing a metric to gauge the biologic response to these new treatments. Gene therapy treatment seeks to correct the underlying pathologic process within the degenerating disc by rebalancing anabolism and catabolism. Our data supported this hypothesis as rabbits treated with AAV2-TIMP1 or AAV2-BMP2 had CTX-II concentrations similar to controls at 12 weeks. The untreated surgical rabbits had a significantly higher CTX-II concentration in comparison to all other groups at the 12-week time point; however, there is still concern that the use of CTX-II to detect the presence and progression of disc degeneration may be confounded by the presence of concomitant degenerative processes such as knee OA as these relationships have not yet been clearly defined. Therefore, future studies will be needed to identify the utility of this marker.

Biomechanics

Because the primary role of the disc is mechanical, assessing the functional response to an intervention requires biomechanical testing. Although both NP and AF are engaged in all forms of loading, axial loading is central to disc function. Compression in the disc is borne primarily by the NP at low frequencies, magnitudes, and durations. Responsibility is

transmitted to the AF with increasing compression. In the ramp phase stiffness analysis, it is apparent that punctured discs lose stiffness relative to controls; BMP2 treatment restores this stiffness, but TIMP1 treatment does not.

Time-dependent mechanical behavior is essential for spinal function. The inherent mechanical properties of the collagen-proteoglycan matrix, interaction of fluid within the solid matrix, and complexity of tissue architecture contribute to FSU viscoelastic behavior. The early viscoelastic response (h1 and S1) is thought to be determined by the NP, whereas the late response (h2 and S2) is thought to be determined by the AF [27]. This may explain why we were able to detect differences in the early response (which is determined by the NP, where interventions in this study were performed) and not in the late response (which is determined by the AF, which was not directly treated in this study). Glycosaminoglycan content (the primary constituent of proteoglycan in the disc), tissue hydration, and fluid exudation through the collagen-proteoglycan matrix govern the viscous parameters, whereas the collagen network determines the elastic parameters [30].

Elastic creep parameters appeared to follow a similar pattern across experimental conditions. Punctured discs decreased somewhat relative to control discs. Tissue inhibitor of metalloproteinase 1 did not seem to influence S2; however, it may have modified S1 in the NP. In contrast, BMP2 clearly increased the elastic parameters in the NP and the AF, suggesting changes in tissue structure or composition relative to punctured discs. Viscous parameters reveal less difference between control and punctured discs, making it difficult to draw conclusions about treatment efficacy. Increases in h1 from BMP2, however, reinforce its potential to alter disc tissue. Although the small sample size precludes statistical certainty and creep durations were shorter than had been used by previous researchers using this model [25,27], this study observes functional changes in the degenerating rabbit lumbar spine and the potential for BMP2 to alter the mechanical properties of the disc.

Spine function comprises active (neuromuscular) and passive (osteoligamentous) subsystems. The primary component of the passive subsystem is the IVD, which supports trunk compression and facilitates trunk motion. The IVD fulfills this mechanical function through unique tissue composition and complex tissue interactions. The solid matrix consists of fixed negatively charged proteoglycans that elicit high osmotic pressures and electrical repulsion, which resists compression. The interstitial fluid of the highly hydrated tissue moves slowly through the dense solid matrix, creating a frictional drag that is responsible for much of the time-varying viscoelastic properties of the disc. The mechanical properties determine how the AF and EPs constrain NP swelling, and their permeabilities regulate the movement of fluid through the disc. Degeneration is known to change the composition and integrity of the solid matrix. The NP dehydrates and becomes more fibrotic, the AF suffers disorganization of collagen sheets and reduced radial permeability, and the EP may deform differently and sclerose. The result is an altered distribution of load and dissipation of energy within the disc and to surrounding structures. These changes may impair spinal function, propagate degeneration along the spinal column, and lead to symptoms. Thus, description of mechanical properties of the disc provides clinically meaningful outcomes that approximate the functional capacity of the disc.

Limitations and directions for future study

The small sample size is typical of other similarly designed studies [14,17,21,31–34]. There were a number of statistically significant findings, and most nonsignificant findings also showed internally consistent trends. This study uses an animal model for degeneration, which does not necessarily translate to the human condition. The annulotomy model is an artificial approximation of human disc degeneration that has similar-appearing MRI and histologic changes. Rabbits are quadrupeds, and the annulotomy model and treatments may behave differently under bipedal conditions. However, there is some biomechanical evidence that viscoelastic properties of rabbit discs under axial load might be translatable to human cadaver discs when normalized to disc size [27]. Detection of BMP2 or TIMP1 gene expression or protein synthesis in the tissue samples would have strengthened this study. Although no adverse effects of treatment were noted, this study does not specifically address the safety of injecting therapeutic genes into the disc (such as overdose, long-term use, misplaced injections, or the possibility of oncogenesis), which is a key concern in weighing the risks and benefits of treating a nonlethal disease such as IDD. Finally, altering the course of disc degeneration by MRI, histologic, serum biochemical, and biomechanical parameters does not necessarily assure that patients would experience any clinically meaningful benefits, such as relief from back and leg pain or improvement in quality of life.

This study used multiple outcome measures, including imaging, histology, biomechanics, and serum biochemistry. Future study should include a biochemical analysis of the disc tissue that quantifies proteoglycan. This may be the keystone to understanding the relationship between all of the other outcomes and, perhaps most interestingly, might help predict whether data from one outcome correlates with data from another. Future directions for investigation should also include elucidating the appropriate timing of injection. Theoretically, an injection would benefit mildly degenerated discs before they become severely and irreversibly damaged; however, the prospect of prophylactically injecting a foreign material into a disc that is only mildly diseased (possibly causing further injury) is a risk that many physicians and patients may be unwilling to take. Finally, a trial application of AAV2-BMP2 and AAV2-TIMP1 gene therapy to real human IDD is a translational research goal.

Conclusions

Based on MRI, histologic, serum biochemical, and biomechanical criteria, injection into the NP of rabbit discs undergoing degeneration via annular puncture with AAV2- BMP2 or AAV2-TIMP1 appears to have a beneficial effect in slowing the degenerative cascade.

Acknowledgments

This work was supported in part by the Albert B. Ferguson, Jr, MD, fund of the Pittsburgh Foundation.

References

1. The Burden of Musculoskeletal Diseases in the United States. Chapter 2: Spine: low back and neck pain. Available at: www.boneandjointburden.org.

2. Fritzell P, Hagg O, Wessberg P, et al. Volvo Award Winner in Clinical Studies: lumbar fusion versus nonsurgical treatment for chronic low back pain: a multicenter randomized controlled trial from the Swedish Lumbar Spine Study Group. Spine. 2001; 26:2521–2534. 2001. [PubMed: 11725230]
3. Park P, Garton H, Gala V, et al. Adjacent segment disease after lumbar or lumbosacral fusion: review of the literature. Spine. 2004; 29:1938–1944. [PubMed: 15534420]
4. Holm S, Maroudas A, Urban J, et al. Nutrition of the intervertebral disc: solute transport and metabolism. Connect Tissue Res. 1981; 8:101–119. [PubMed: 6453689]
5. Bradford D, Cooper K, Oegema T. Chymopapain, chemonucleolysis, and nucleus pulposus regeneration. J Bone Joint Surg Am. 1983; 65:1220–1231. [PubMed: 6361035]
6. Pearce R, Grimmer B, Adams M. Degeneration and the chemical composition of the human intervertebral disc. J Orthop Res. 1987; 5:198–205. [PubMed: 3572589]
7. Urban J, McMullen J. Swelling pressure of the intervertebral disc: influence of proteoglycan and collagen contents. Biorheology. 1985; 22:145–157. [PubMed: 3986322]
8. Li J, Kim K, Park J, et al. BMP-2 and CDMP-2: stimulation of chondrocyte production of proteoglycan. J Orthop Sci. 2003; 8:829–835. [PubMed: 14648273]
9. Li J, Yoon T, Hutton W. Effect of bone morphogenetic protein-2 (BMP-2) on matrix production, other BMPs, and BMP receptors in rat intervertebral disc cells. J Spinal Disord Tech. 2004; 17:423–428. [PubMed: 15385883]
10. Kanemoto M, Hukuda S, Komiya Y, et al. Immunohistochemical study of matrix metalloproteinase-3 and tissue inhibitor of metalloproteinase-1 in human intervertebral discs. Spine. 1996; 21:1–8. [PubMed: 9122749]
11. Wallach C, Sobajima S, Watanabe Y, et al. Gene transfer of the catabolic inhibitor TIMP-1 increases measured proteoglycans in cells from degenerated human intervertebral discs. Spine. 2003; 28:2331–2337. [PubMed: 14560079]
12. Driesse M, Esandi M, Kros J, et al. Intra-CSF administered recombinant adenovirus causes an immune response-mediated toxicity. Gene Ther. 2000; 7:1401–1409. [PubMed: 10981667]
13. Levicoff E, Kim S, Sobajima S, et al. Safety assessment of intradiscal gene therapy II: effect of dosing and vector choice. Spine. 2008; 33:1509–1516. [PubMed: 18520636]
14. Latterman C, Oxner W, Xiao X, et al. The adeno associated viral vector as a strategy for intradiscal gene transfer in immune competent and pre-exposed rabbits. Spine. 2005; 30:497–504. [PubMed: 15738780]
15. Kim H, Viggeswarapu M, Boden S. Overcoming the immune response to permit ex vivo gene therapy for spine fusion with human type 5 adenoviral delivery of the LIM mineralization protein-1 cDNA. Spine. 2003; 28:219–226. [PubMed: 12567021]
16. Afione S, Wang J, Walsh S, et al. Delayed expression of adeno-associated virus vector DNA. Intervirology. 1999; 42:213–220. [PubMed: 10567839]
17. Masuda K, Aota Y, Muehlman C, et al. A novel rabbit model of mild, reproducible disc degeneration by anulus needle puncture: correlation between the degree of disc injury and radiological and histological appearances of disc degeneration. Spine. 2005; 30:5–14. [PubMed: 15626974]
18. Xiao X, Li J, Samulski R. Production of high-titer recombinant adeno-associated virus vector in the absence of helper adenovirus. J Virol. 1998; 72:2224–2232. [PubMed: 9499080]
19. Wang B, Li J, Xiao X. Adeno-associated virus vector carrying human minidystrophin genes effectively ameliorates muscular dystrophy in mdx mouse model. Proc Natl Acad Sci U S A. 2000; 25:13714–13719. [PubMed: 11095710]
20. Tang Y, Reay D, Salay M, et al. Inhibition of the IKK/NF-κB pathway by AAV gene transfer improves muscle regeneration in older mdx mice. Gene Ther. 2010; 17:1476–1483. [PubMed: 20720575]
21. Sobajima S, Kompel J, Joseph K, et al. A slowly progressive and reproducible animal model of intervertebral disc degeneration characterized by MRI, X-ray, and histology. Spine. 2005; 30:15–24. [PubMed: 15626975]
22. Elliott D, Yerramalli C, Beckstein J, et al. The effect of relative needle diameter in puncture and sham injection animal models of degeneration. Spine. 2008; 33:588–596. [PubMed: 18344851]

23. An H, Takegami K, Kamada H, et al. Intradiscal administration of osteogenic protein-1 increases intervertebral disc height and proteoglycan content in the nucleus pulposus in normal adolescent rabbits. Spine. 2005; 30:25–31. [PubMed: 15626976]
24. Sowa G, Westrick E, Pacek C, et al. In vitro and in vivo testing of a novel regulatory system for gene therapy for intervertebral disc degeneration. Spine. 2011; 36:623–628.
25. Bechara B, Leckie S, Bowman B, et al. Application of a semi-automated contour segmentation tool to identify the intervertebral nucleus pulposus in MR images. Am J Neuroradiol. 2010; 31:1640–1644. [PubMed: 20581067]
26. Sowa G, Westrick E, Rajasekhar A, et al. Identification of candidate serum biomarkers for intervertebral disk degeneration in an animal model. PM R. 2009; 1:536–540. [PubMed: 19627943]
27. Beckstein J, Sen S, Schaer T, et al. Comparison of animal discs used in disc research to human lumbar discs: axial compression mechanics and glycosaminoglycan content. Spine. 2008; 33:E166–E173. [PubMed: 18344845]
28. Wilke H-J, Neef P, Caimi M, et al. New in vivo measurements of pressures in the intervertebral disc in daily life. Spine. 1999; 24:755–762. [PubMed: 10222525]
29. Johannessen W, Cloyd J, O'Connell G, et al. Trans-endplate nucleotomy increases deformation and creep response in axial loading. Ann Biomed Eng. 2006; 34:687–696. [PubMed: 16482409]
30. Boxberger J, Sen S, Yerramalli C, Elliot D. Nucleus pulposus glycosaminoglycan content is correlated with axial mechanics in rat lumbar motion segments. J Orthop Res. 2006; 24:1906–1915. [PubMed: 16865712]
31. Masuda K, Imai Y, Okuma M, et al. Osteogenic protein-1 injection into a degenerated disc induces the restoration of disc height and structural changes in the rabbit annular puncture model. Spine. 2006; 31:742–754. [PubMed: 16582847]
32. Imai Y, Okuma M, An H, et al. Restoration of disc height loss by recombinant human osteogenic protein-1 injection into intervertebral discs undergoing degeneration induced by an intradiscal injection of chondroitinase ABC. Spine. 2007; 32:1197–1205. [PubMed: 17495776]
33. Yoon S, Park J, Kim K, et al. ISSLS prize winner: LMP-1 upregulates intervertebral disc cell production of proteoglycans and BMPs in vitro and in vivo. Spine. 2004; 29:2603–2611. [PubMed: 15564908]
34. Nishida K, Kang J, Gilbertson L, et al. Volvo Award Winner in Basic Science Studies: modulation of the biological activity of the rabbit intervertebral disc by gene therapy: an in vivo study of adenovirus-mediated transfer of the human transforming growth factor beta 1 encoding gene. Spine. 1999; 24:2419–2425. 1999. [PubMed: 10626303]
35. Paul R, Haydon R, Cheng H, et al. Potential use of Sox9 gene therapy for intervertebral degenerative disc disease. Spine. 2003; 28:755–763. [PubMed: 12698117]
36. Vadala G, Sowa G, Smith L, et al. Regulation of transgene expression using an inducible system for improved safety of intervertebral disc gene therapy. Spine. 2007; 32:1381–1387. [PubMed: 17545904]
37. Kim S, Yoon T, Li J, et al. Disc degeneration in the rabbit: a biochemical and radiological comparison between four disc injury models. Spine. 2004; 30:33–37. [PubMed: 15626978]
38. Benneker L, Heini P, Anderson S, et al. Correlation of radiographic and MRI parameters to morphological and biochemical assessment of intervertebral disc degeneration. Eur Spine J. 2005; 14:27–35. [PubMed: 15723249]
39. Sowa G, Vadala G, Studer R, et al. Characterization of intervertebral disc aging: longitudinal analysis of a rabbit model by magnetic resonance imaging, histology, and gene expression. Spine. 2008; 33:1821–1828. [PubMed: 18670334]
40. Haig A, Tong H, Yamakawa K, et al. Spinal stenosis, back pain, or no symptoms at all? A masked study comparing radiologic and electrodiagnostic diagnoses to the clinical impression. Arch Phys Med Rehabil. 2006; 87:897–903. [PubMed: 16813774]
41. Pfirrmann C, Metzdorf A, Elfering A, et al. Effect of aging and degeneration on disc volume and shape: a quantitative study in asymptomatic volunteers. J Orthop Res. 2006; 24:1086–1094. [PubMed: 16609964]

42. van Rijn J, Klemetso N, Reitsma J, et al. Symptomatic and asymptomatic abnormalities in patients with lumbosacral radicular syndrome: clinical examination compared with MRI. Clin Neurol Neurosurg. 2006; 108:553–557. [PubMed: 16289310]
43. Bono C, Lee C. Critical analysis of trends in fusion for degenerative disc disease over the past 20 years: influence of technique on fusion rate and clinical outcome. Spine. 2004; 29:455–463. discussion Z455. [PubMed: 15094543]
44. Jordan K, Syddall H, Garnero P, et al. Urinary CTX-II and glucosyl-galactosyl-pyridinoline are associated with the presence and severity of radiographic knee osteoarthritis in men. Ann Rheum Dis. 2006; 65:871–877. [PubMed: 16284096]
45. Masuhara K, Nakai T, Yamaguchi K, et al. Significant increases in serum and plasma concentrations of matrix metalloproteinases 3 and 9 in patients with rapidly destructive osteoarthritis of the hip. Arthritis Rheum. 2002; 46:2625–2631. [PubMed: 12384920]
46. Mahmoud R, El-Ansary A, El-Eishi H, et al. Matrix metalloproteinases MMP-3 and MMP-1 levels in sera and synovial fluids in patients with rheumatoid arthritis and osteoarthritis. Ital J Biochem. 2005; 54:248–257. [PubMed: 16688934]
47. Egerer K, Hertzer J, Feist E, et al. E-selectin for stratifying outcome in rheumatoid arthritis. Arthritis Rheum. 2003; 49:546–548. [PubMed: 12910562]
48. Garnero P, Sornay-Rendu E, Arlot M, et al. Association between spine disc degeneration and type II collagen degradation in postmenopausal women. Arthritis Rheum. 2004; 50:3137–3144. [PubMed: 15476251]
49. Garnero P, Charni N, Juillet F, et al. Increased urinary type II collagen helical and C telopeptide levels are independently associated with a rapidly destructive hip osteoarthritis. Ann Rheum Dis. 2006; 65:1639–1644. [PubMed: 16569684]
50. Poole A. Biologic markers and disc degeneration. J Bone Joint Surg Am. 2006; 88(Suppl 2):72–75. [PubMed: 16595448]
51. Zolotukhin S, Potter M, Hauswirth W, et al. A “humanized” green fluorescent protein cDNA adapted for high-level expression in mammalian cells. J Virol. 1996; 70:4646–4654. [PubMed: 8676491]
52. Wang Z, Ma H, Li J, et al. Rapid and highly efficient transduction by double-stranded adeno-associated virus vectors in vitro and in vivo. Gene Ther. 2003; 10:2105–2111. [PubMed: 14625564]

Time	Control N=6	Sham Surgery N=4	Puncture N=7	AAV2-BMP2 N=8	AAV2-TIMP1 N=8
0 wk	MRI Serum	MRI Serum Sham surgery	MRI Serum Puncture surgery -L2–L3, L3–L4, L4–L5	MRI Serum Puncture surgery -L2–L3, L3–L4, L4–L5	MRI Serum Puncture surgery -L2–L3, L3–L4, L4–L5
3 wk				Injection surgery -L2–L3, L3–L4, L4–L5 -10^8 VP/15 μL/disc	Injection surgery -L2–L3, L3–L4, L4–L5 -10^8 VP/15 μL/disc
6 wk	MRI Serum	MRI Serum	MRI Serum	MRI Serum	MRI Serum
12 wk	MRI Serum Sacrifice -Histo L4–5 -BioM L3–4	MRI Serum Sacrifice -Histo L4–5 -BioM L3–4	MRI Serum Sacrifice -Histo L4–5 -BioM L3–4	MRI Serum Sacrifice -Histo L4–5 -BioM L3–4	MRI Serum Sacrifice -Histo L4–5 -BioM L3–4

Fig. 1.
Project overview. MRI, magnetic resonance imaging; VP, virus particle; Histo, histology; BioM, biomechanics.

Fig. 2.

Construction of recombinant adeno-associated virus (AAV) vectors. Schematic illustration of two AAV vectors containing the human bone morphogenetic protein 2 (hBMP2) gene and human tissue inhibitor of metalloproteinase 1 (hTIMP1) gene were constructed as described. Both vectors were controlled by the human cytomegalovirus (CMV) immediate-early promoter/enhancer and followed by the simian virus 40 polyadenylation signal (SV40_pA). The difference between two vectors is that the BMP2 gene (1,191 bp) was cloned into a single-stranded AAV vector [51], and the complementary DNA of TIMP1 (624 bp) was cloned into a self-complementary AAV vector [52]. ITR, inverted terminal repeat; Pcmv, human cytomegalovirus immediate-early promoter/enhancer; SD/SA, the SV40 late viral protein gene 16s/19s splice donor and acceptor signals; POenh, a tandem repeat of the enhancer from the polymavirus mutant PYF441; Ptk, the thymidine kinase promoter of herpes simplex virus; neor, the neomycin gene from Tn5; Bgh_pA, the bovine growth hormone polyadenylation signal from pRc/CMV (Invitrogen); 6ITR, mutant ITR.

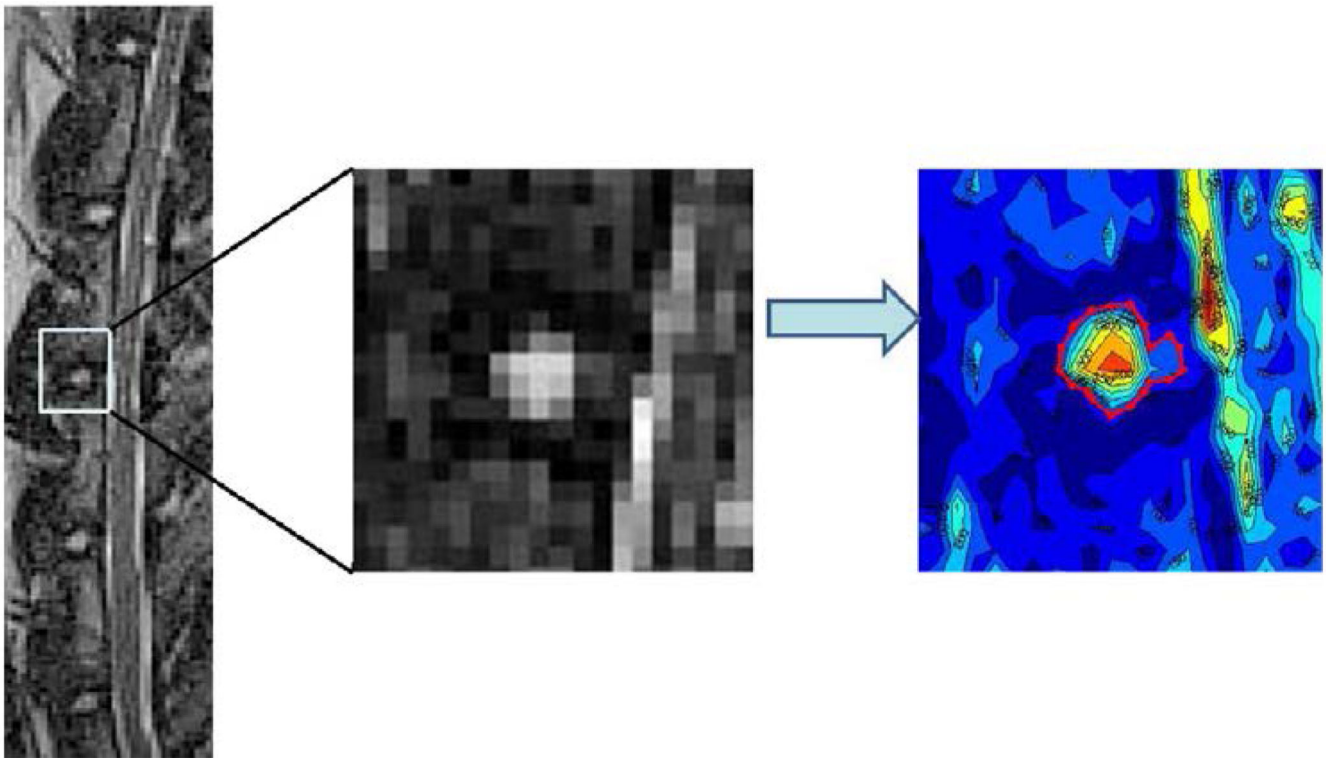

Fig. 3.

Contour segmentation. (Left) Midsagittal T2-weighted magnetic resonance imaging of the lumbar spine at time point 0 and (Middle) magnified image of the L3–L4 disc. A previously validated automated computer program applies signal intensity isolines to the area around each disc. (Right) The largest concentric circle, representing the nucleus pulposus, is selected as the region of interest.

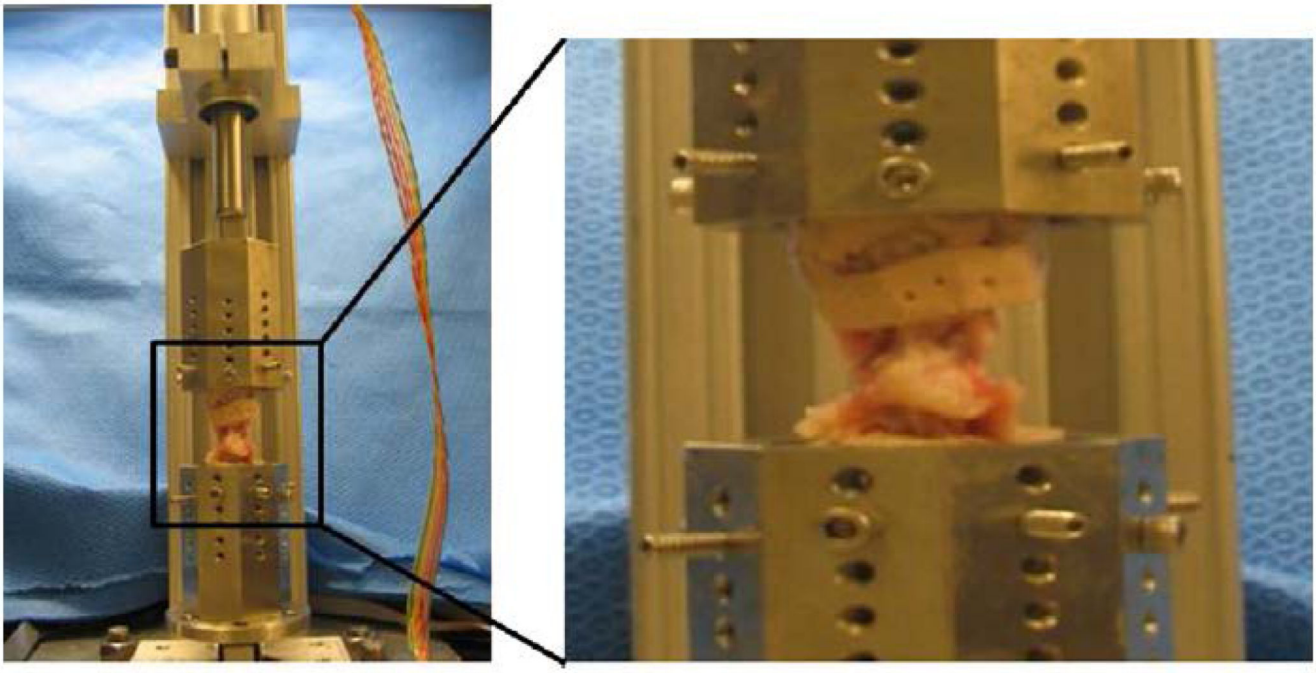

Fig. 4.
Biomechanics robot. (Left) Photograph of the axial testing robot used for biomechanical analysis. (Right) Zoomed in photograph of a potted L3–L4 functional spinal unit.

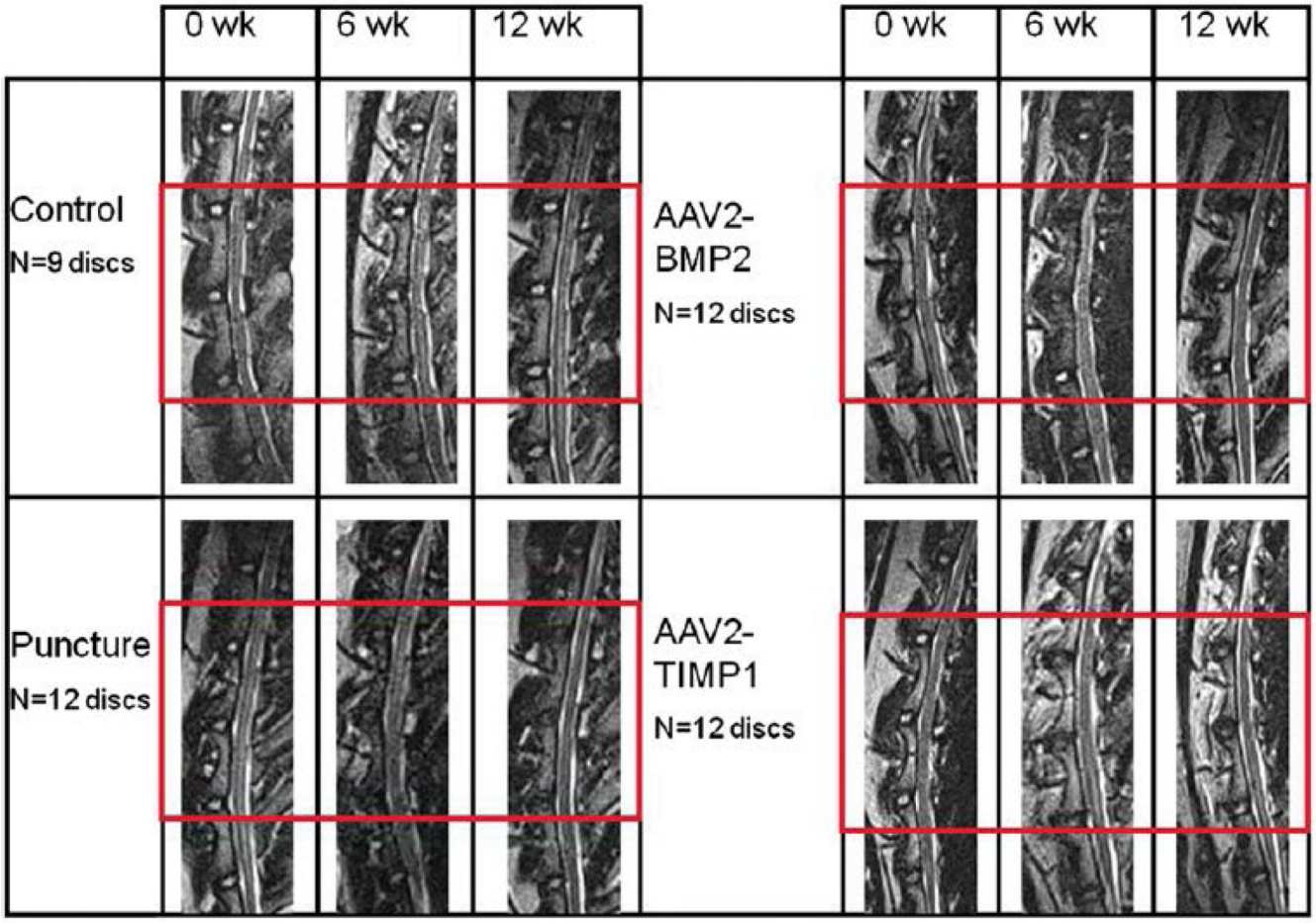

Fig. 5.

Lumbar spine magnetic resonance imaging (MRI) studies. Sample T2-weighted midsagittal lumbar MRIs of L1–L2 through L5–L6 at time points 0, 6, and 12 weeks. The treated discs (L2–L3, L3–L4, and L4–L5) are outlined by the red box. Sham surgery discs (not shown) look like nonpunctured control discs. AAV2-BMP2, adeno-associated virus serotype 2-bone morphogenetic protein 2; AAV2-TIMP1, adeno-associated virus serotype 2-tissue inhibitor of metalloproteinase 1.

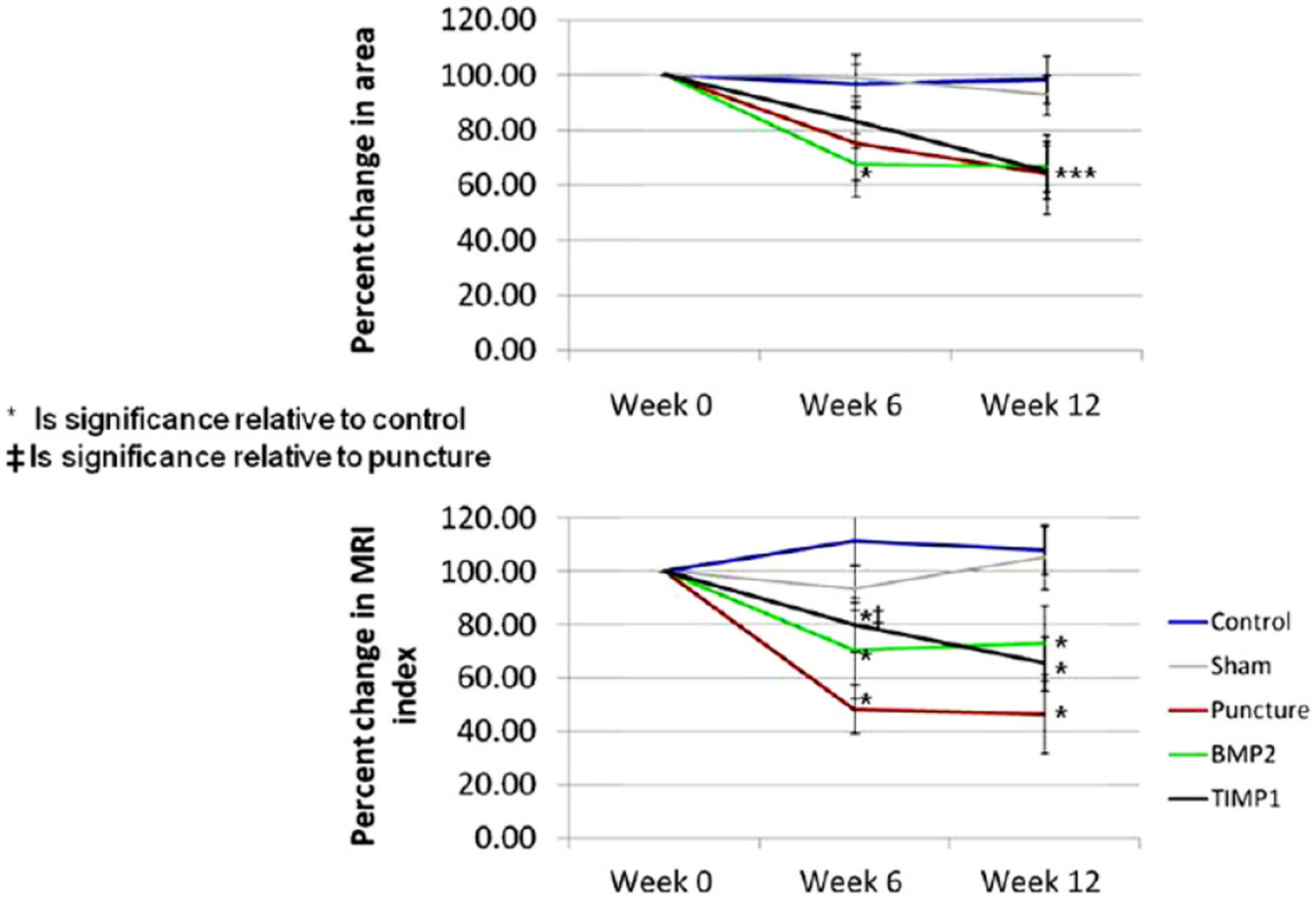

Fig. 6.

T2-weighted magnetic resonance imaging (MRI) nucleus pulposus (NP) area and MRI index. Contour segmentation of the midsagittal MRI for each disc outlined the NP as the region of interest. (Top) Average data for NP area and (Bottom) MRI index combining L2–L3, L3–L4, and L4–L5 (the treated discs) for each rabbit group are expressed as a percent of the time 0 value. Error bars represent standard error. BMP2, bone morphogenetic protein 2; TIMP1, tissue inhibitor of metalloproteinase 1.

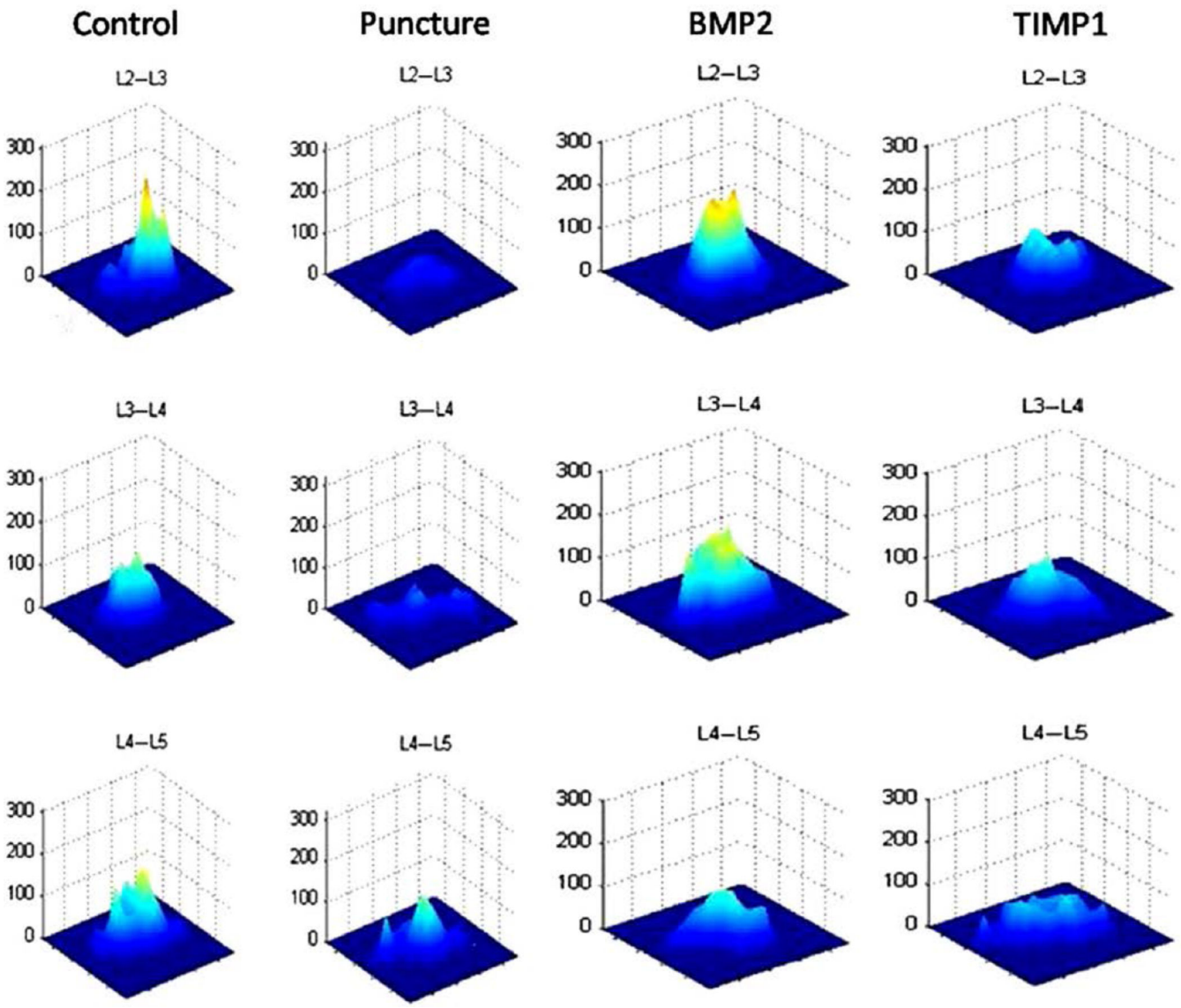

Fig. 7.

T2 maps. The midsagittal magnetic resonance image is selected for each disc, and a contour segmentation program outlines the disc space as the region of interest. Signal intensity for each pixel across echo times (12, 24, 36, 48, and 60 ms) is plotted on the vertical axis, with the distance from the center of the disc plotted on the horizontal axis. The slope of the map reflects disc degeneration. A steeper slope represents a greater contrast between bright and dark signal intensity within the disc, demonstrating relative heterogeneity within the nondegenerated disc. A flatter slope represents a decreased contrast between bright and dark signal intensity in the disc demonstrating relative homogeneity (suggestive of degeneration). Representative T2 maps obtained at 12 weeks are depicted.

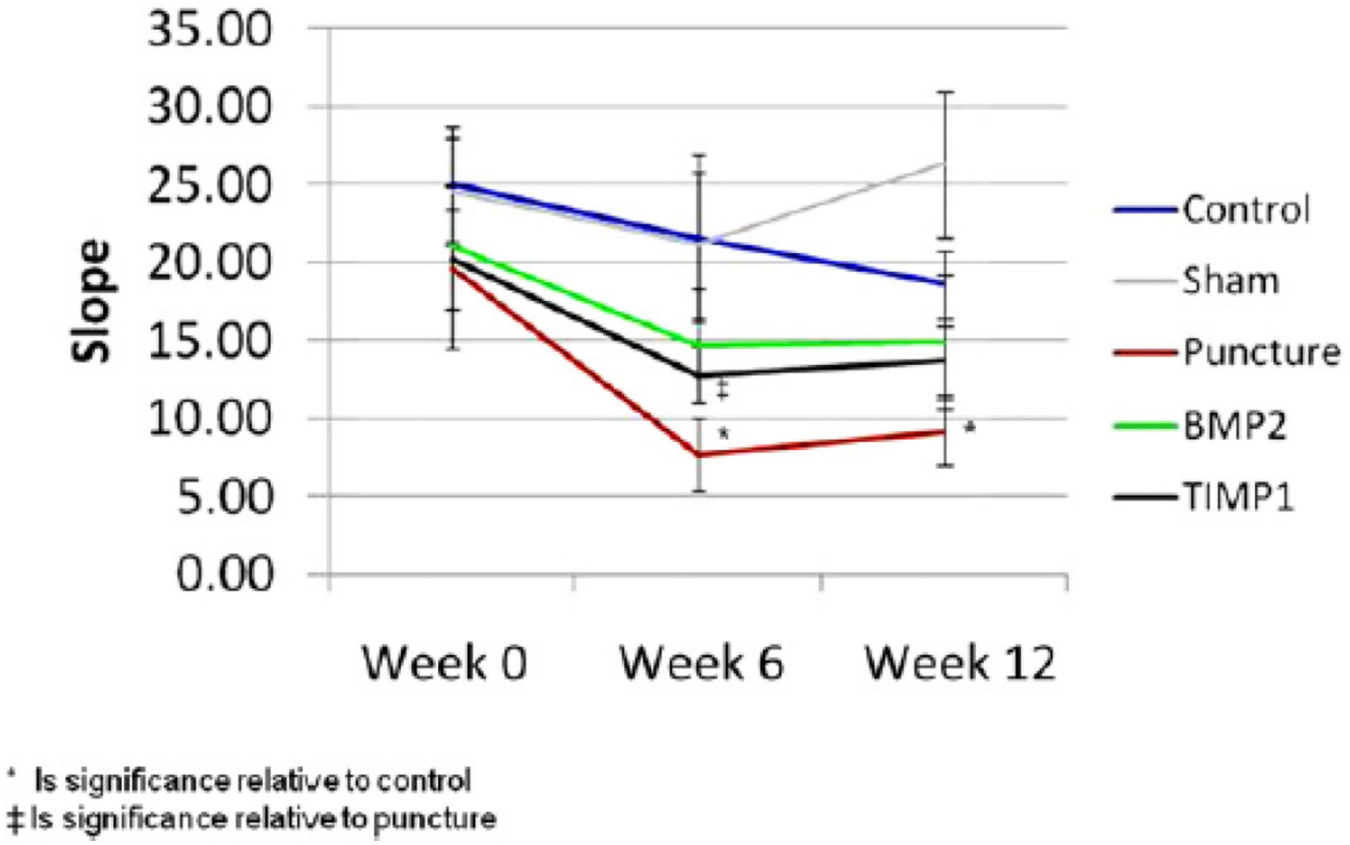

Fig. 8.

T2 map slopes. Average map slopes for discs L2–L3, L3–L4, and L4–L5 for each group, at 0, 6, and 12 weeks. Error bars represent standard error.

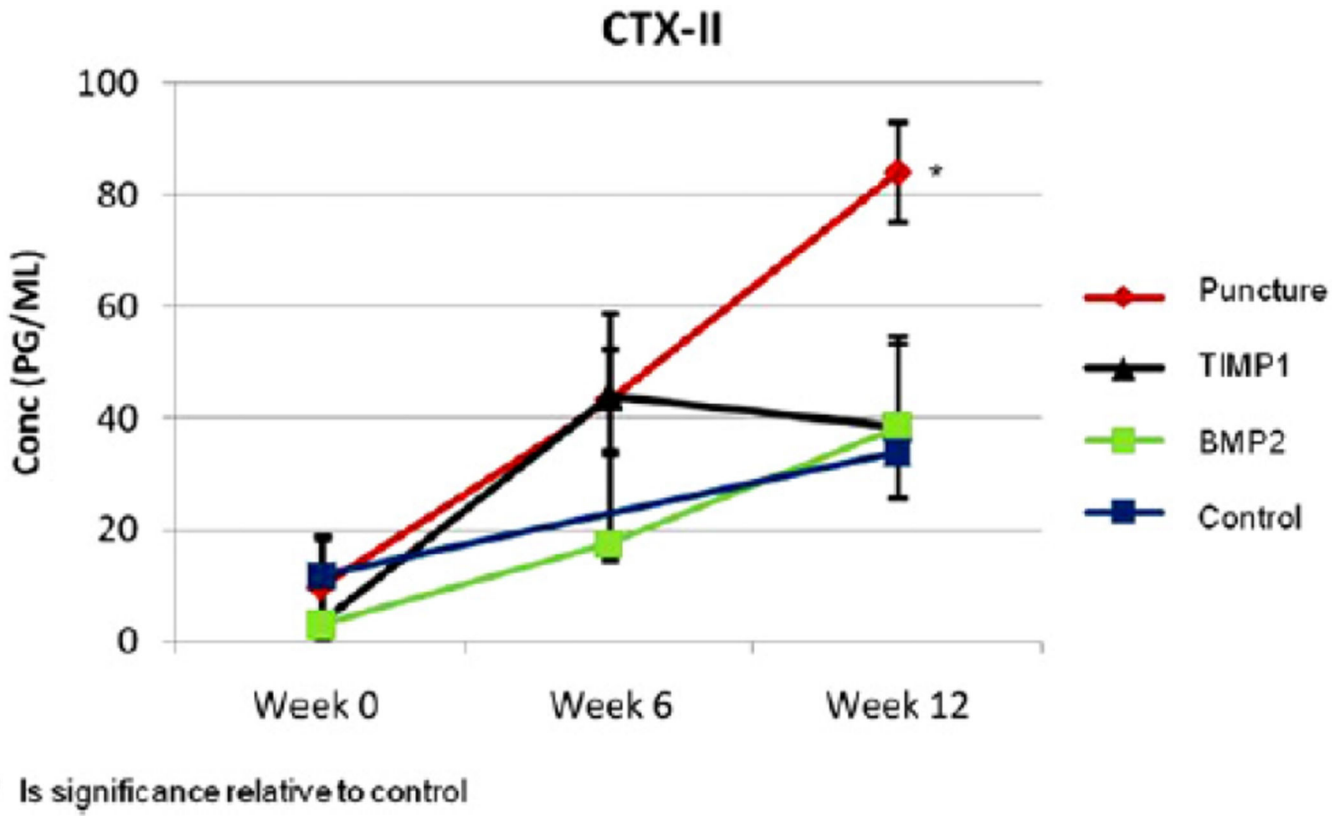

Fig. 9.

Serum analysis C-telopeptide of collagen Type II serum concentrations for each group across time points 0 (before puncture surgery), 6, and 12 weeks.

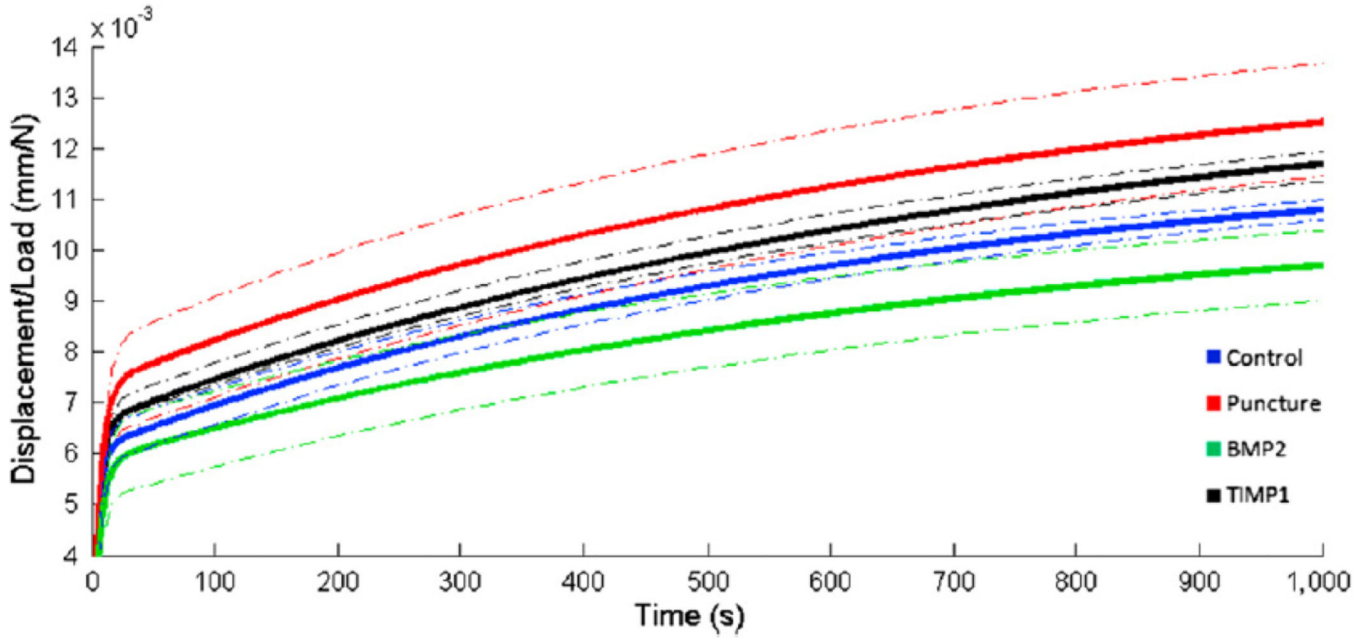

Fig. 10.

Average normalized total displacement (ramp phaseþcreep) curves. After sacrifice at 12 weeks, functional spinal units for L3–L4 were potted in an axial testing robot. Specimens were preconditioned and then subjected to constant compression. Average load-normalized displacement curves were generated for each condition. Dotted lines represent one standard deviation within each treatment group.

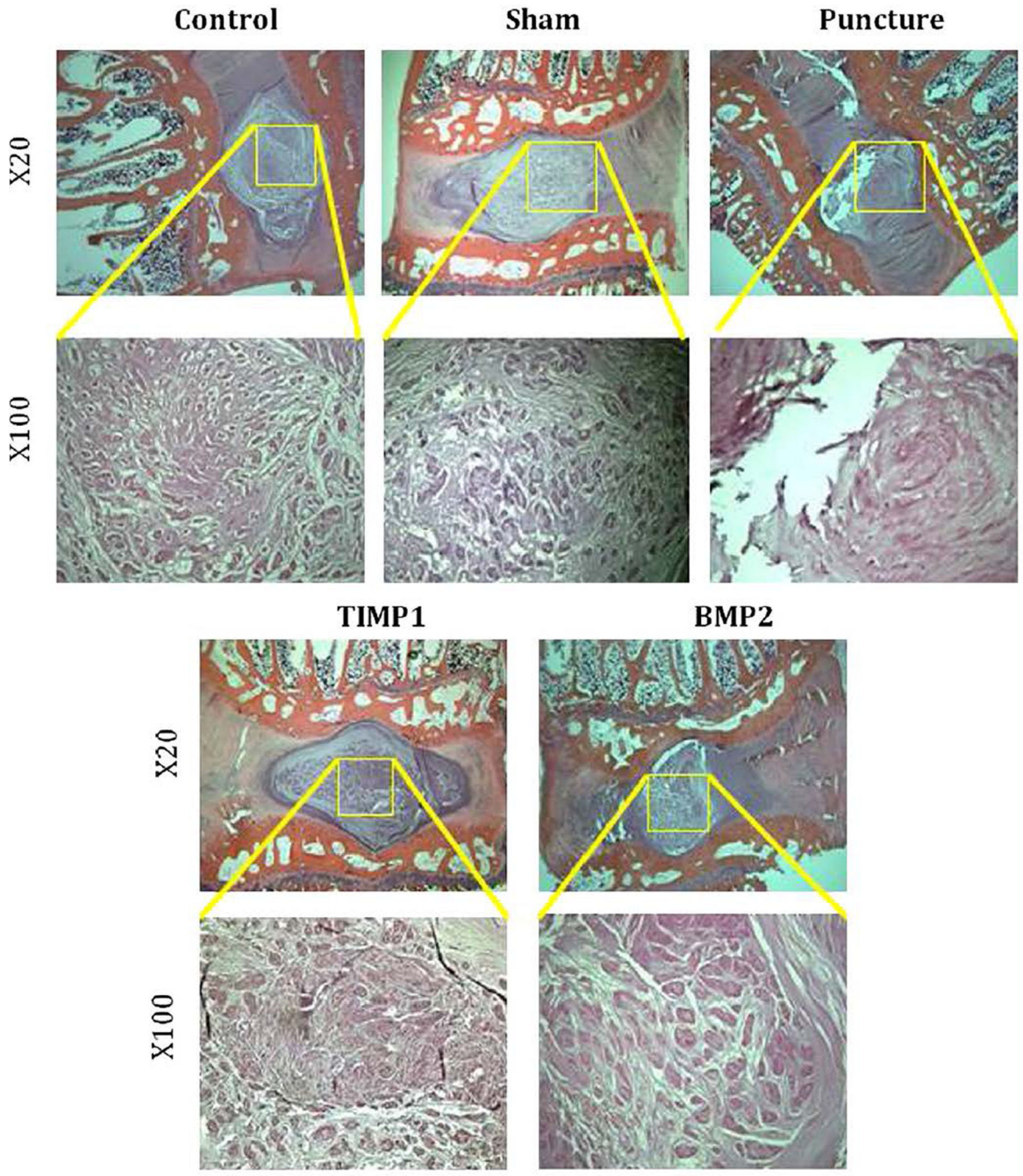

Fig. 11.

Histology: Midsagittal slices of L4–L5 obtained after sacrifice at 12 weeks, stained with hematoxylin and eosin, and magnified 20× and 100×.

Table

Stiffness and damping coefficients

Group	k (N/mm)	S_1 (N/mm)	S_2 (N/mm)	η_1 (Ns/mm)	η_2 (Ns/mm)
Control	280.9 (41.0)	819.3	170.0	26364.6	132333.0
Puncture	249.1 (49.7)	683.9	145.4	29031.7	132682.2
Bone morphogenetic protein 2	287.4 (58.5)	887.5	201.9	31041.7	160556.8
Tissue inhibitor of metalloproteinase 1	238.3 (11.4)	780.1	149.1	24857.3	125341.4

Mechanical properties: Ramp phase stiffness (k) and viscoelastic model damping coefficients (elastic: S_1, S_2; viscous: η_1, η_2). The top ≈ 30% of the linear region of the ramp phase was used for stiffness calculations. Damping coefficient parameters are derived from average curves. Creep curves were fit with a two-phase exponential model, where S_1 describes the early elastic damping coefficient, S_2 describes the late elastic damping coefficient, η_1 describes the early viscous damping coefficient, and η_2 describes the late viscous damping coefficient.